

# PPy Enhanced Fe, W Co-doped Co<sub>3</sub>O<sub>4</sub> Free-Standing Electrode for Highly-Efficient Oxygen Evolution Reaction

*Qingzhao Hu<sup>a</sup>, Yan Liu<sup>a</sup>, Longtao Ma<sup>b</sup>, Xuming Zhang<sup>a</sup>, Haitao Huang<sup>\*a</sup>*

*<sup>a</sup> Department of Applied Physics, The Hong Kong Polytechnic University, Hung Hom,  
Kowloon, Hong Kong, 999077, China*

*<sup>b</sup> Department of Materials Science and Engineering, City University of Hong Kong,  
Kowloon, Hong Kong, 999077, China*

*\*Corresponding author:*

*E-mail address: [aphhuang@polyu.edu.hk](mailto:aphhuang@polyu.edu.hk)*

## Abstract

Electrochemical catalysts for the oxygen evolution reaction (OER) play a key role in highly-efficient water splitting and many other important energy conversion applications. Transition metal oxides are promising OER catalysts. In this work, Fe,W co-doped  $\text{Co}_3\text{O}_4$  was grown on carbon fiber cloth ( $\text{FeWCo}_3\text{O}_4/\text{CFC}$ ) and polypyrrole (PPy)/carbon fiber cloth ( $\text{FeWCo}_3\text{O}_4/\text{PPy}/\text{CFC}$ ) through a simple anodic electrodeposition method. The  $\text{FeWCo}_3\text{O}_4/\text{CFC}$  free-standing electrode reached an electrocatalytic current density of  $30.7 \text{ mA cm}^{-2}$  at 400 mV overpotential with a Tafel slope of  $177 \text{ mV dec}^{-1}$ . The PPy can serve as conductive binder and improve the contact between  $\text{FeWCo}_3\text{O}_4$  and substrate. The resulting  $\text{FeWCo}_3\text{O}_4/\text{PPy}/\text{CFC}$  free-standing electrode reached an electrocatalytic current density of  $36.2 \text{ mA cm}^{-2}$  at 400 mV overpotential with a Tafel slope of  $163 \text{ mV dec}^{-1}$ . The  $\text{FeWCo}_3\text{O}_4/\text{PPy}/\text{CFC}$  free-standing electrode shows low electric resistance and is able to catalyze OER at  $10 \text{ mA cm}^{-2}$  for 12 hours without obvious decay under the optimized electrodeposition conditions. This study provides new insight for design and synthesis of highly-efficient OER catalyst.

Keywords: Oxygen evolution reaction; Free-standing electrode; Electrodeposition: PPy

## Introduction

Energy crisis and global warming have raised worldwide interest in developing environment-friendly energy sources [1-3]. Alternatives to fossil fuels are significant to help reduce green-house effect and air pollution [4,3]. Hydrogen, which is recognized as a clean and renewable energy source, possesses great potential to become the next generation energy source [2,3]. Hydrogen production through methane or coal in industry involves enormous carbon dioxide emission [5]. While mass production of hydrogen by electrolysis with high efficiency remains laborious due to the sluggish kinetics of oxygen evolution reaction (OER) in water splitting [5,6]. Superb catalyst which can promote the oxygen evolution is crucial to the production of hydrogen through water splitting. The state-of-art catalysts  $\text{RuO}_2$  and  $\text{IrO}_2$  suffer from high cost and low abundance [7]. Catalyst fabricated with earth-abundant elements is therefore needed to surmount the reaction obstacles and increase the efficiency.

Recent years have seen huge efforts focused on the synthesis of transition metal-based materials [8-15], such as transition metal oxides and transition metal (oxy)hydroxides ( $\text{CoOOH}$  [16],  $\text{NiCoFe}$  layered triple hydroxide [17],  $\text{FeCoW}$  oxyhydroxide [9]), transition metal phosphides ( $\text{CoP}$  [18],  $\text{NiP}$  [19]), metal-organic frameworks ( $\text{NiCo}$  bimetal-organic framework [20]) and composites ( $\text{NiFe}$  layered double hydroxide-graphene oxide [8]). Some OER catalysts derived from  $\text{Co}_3\text{O}_4$  have been reported, such as  $\text{Au@Co}_3\text{O}_4$  core-shell nanocrystals [21] and graphene- $\text{Co}_3\text{O}_4$  nanocomposite [22]. However, the synthesis of  $\text{Au@Co}_3\text{O}_4$  core-shell nanocrystals involves noble metal, which is adverse to industry application. The synthesis method

of graphene-Co<sub>3</sub>O<sub>4</sub> nanocomposite is complicated and high temperature calcination is also required. In addition, binder such as Nafion is needed for the fabrication of electrodes using powdered catalysts [23,20]. Therefore, the fabrication of free-standing electrode with highly-efficient OER catalysts that consist of earth-abundant elements is attractive and challenging.

There are two general approaches to the development of an effective catalyst: improving the intrinsic property of each site or increasing the amount of effective sites. Intrinsic property can be enhanced by tuning binding energies of reaction intermediates. Morphology design contributes to the number of effective active sites [15]. A recent study predicted the superior intrinsic catalytic performance of FeCoW oxyhydroxide by calculating the corresponding binding energies of the intermediates using density functional theory (DFT+U) [9]. Non-3d high-valency metals such as tungsten can modulate 3d metal oxides to provide optimized adsorption energies and electronic structure for highly efficient OER. Cobalt-based composites supported on carbon fiber substrate are shown to be highly-efficient electrochemical catalysts, which may result from high electric conductivity and synergistic effect between cobalt oxide/cobalt and carbon substrate.[24,25] It is reported that PPy/carbon structure can increase the metal availability for electrode reaction.[26] Meanwhile, PPy and cobalt can form Co-N active sites with enhanced electrochemical property.[27,28] Therefore, a highly-efficient OER catalytic electrode is expected through the fabrication of FeCoW catalyst supported by PPy/CFC substrate.

Herein, FeWCo<sub>3</sub>O<sub>4</sub>/PPy/CFC free-standing electrode was synthesized through a

simple electrodeposition method and showed efficient OER catalytic performance. The FeWCo<sub>3</sub>O<sub>4</sub>/PPy/CFC electrodes achieved a higher current density (36.2 mA cm<sup>-2</sup>) than FeWCo<sub>3</sub>O<sub>4</sub>/CFC (30.7 mA cm<sup>-2</sup>) at an overpotential of 400 mV. The PPy was demonstrated to improve the contact between active material and substrate, which enables better OER electrocatalytic performance of FeWCo<sub>3</sub>O<sub>4</sub>/PPy/CFC electrode than that of FeWCo<sub>3</sub>O<sub>4</sub>/CFC electrode.

## Experimental section

Carbon fiber clothes (CFC) were firstly washed with deionized water (DI water) and acetone several times, then immersed into dilute nitric acid for 24 hours to remove the surface impurities. Thereafter, the CFC were washed with DI water and dried at 60 °C in oven for 2 hours before use.

### *PPy grown on CFC (PPy/CFC)*

Pyrrole (1 mL) was firstly dissolved into DI water (50 mL). Then ammonium persulfate (1 g) and sodium p-toluenesulfonate (1 g) were added into the above solution. Thereafter the solution was placed into ice bath and stirred for 10 mins. CFC were put into the solution for 2 hours' polymerization to obtain PPy/CFC, which was then washed with DI water several times and dried in oven at 60 °C for 2 hours.

### *Fe, W co-doped Co<sub>3</sub>O<sub>4</sub> grown on PPy/CFC (FeWCo<sub>3</sub>O<sub>4</sub>/PPy/CFC)*

Trisodium citrate dehydrate (14.75 g), boric acid (2.56 g), sodium tungstate (19.5 g), Iron(II) chloride tetrahydrate (0.49 g) and cobalt chloride hexahydrate (0.59 g) were dissolved into DI water (250 mL). Phosphoric acid (1.9 mL, 85 wt%) was added into the above solution. Then the solution was put under ultrasonic condition for 1 hour. After that, the solution was stirred for 12 hours to become homogenous. The above solution was added into an electrochemical cell with PPy/CFC as anode, Pt plate as cathode. Electrodeposition was conducted under a constant current density of 40 mA cm<sup>-2</sup> for 2 hours under 60 °C water bath condition. The deposited FeWCo<sub>3</sub>O<sub>4</sub>/PPy/CFC

was washed with DI water and ethanol for several times. Scheme 1 shows the synthesis of FeWCo<sub>3</sub>O<sub>4</sub>/PPy/CFC schematically.

#### *Fe, W co-doped Co<sub>3</sub>O<sub>4</sub> grown on CFC (FeWCo<sub>3</sub>O<sub>4</sub>/CFC)*

The method used was similar to that of the deposition of FeWCo<sub>3</sub>O<sub>4</sub>/PPy/CFC with CFC being the anode instead of PPy/CFC.

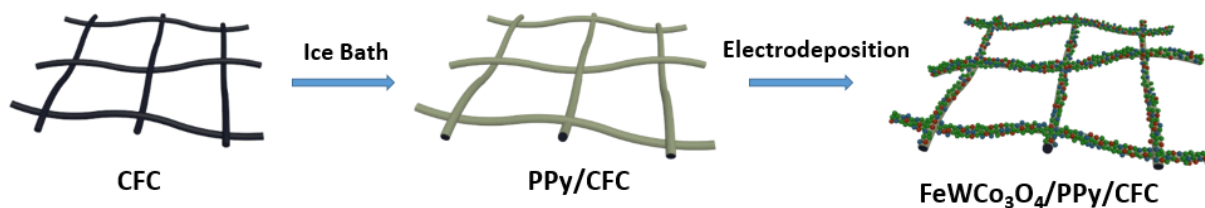
#### Characterizations

Scanning electron microscope (SEM, TM 3000, Hitachi, Japan) and transmission electron microscopy (TEM, JOEL JEM-2010, Japan) were used for microstructure and morphology characterizations. X-ray Diffraction (XRD, Rigaku D/max IIIA, Cu K $\alpha$ ,  $\lambda=0.15418$  nm, Japan) was used for crystalline structure analysis. Raman spectrum was conducted on a HORIBA Raman spectrometer at 488 nm. X-ray photoelectron spectroscopy (XPS, Thermo Microlab 350) was used to study the surface composition of FeWCo<sub>3</sub>O<sub>4</sub> inside an ultrahigh vacuum system.

#### Electrochemical Measurements

Linear sweep voltammetry (LSV), cyclic voltammetry (CV), electrochemical impedance spectroscopy (EIS, 0.01-1000k Hz frequency) and chronopotentiometric tests were performed on an electrochemical workstation (Solartron Analytical 1470E). A classical three-electrode configuration was used with Pt plate as counter electrode and saturated calomel electrode (SCE) as reference electrode. The measurement was conducted in 1 mol L<sup>-1</sup> KOH solution and the polarization curve was tested at a scan rate of 2 mV s<sup>-1</sup>.

## Results & Discussion



**Scheme 1.** Schematic illustration of synthesis of FeWCo<sub>3</sub>O<sub>4</sub>/PPy/CFC.

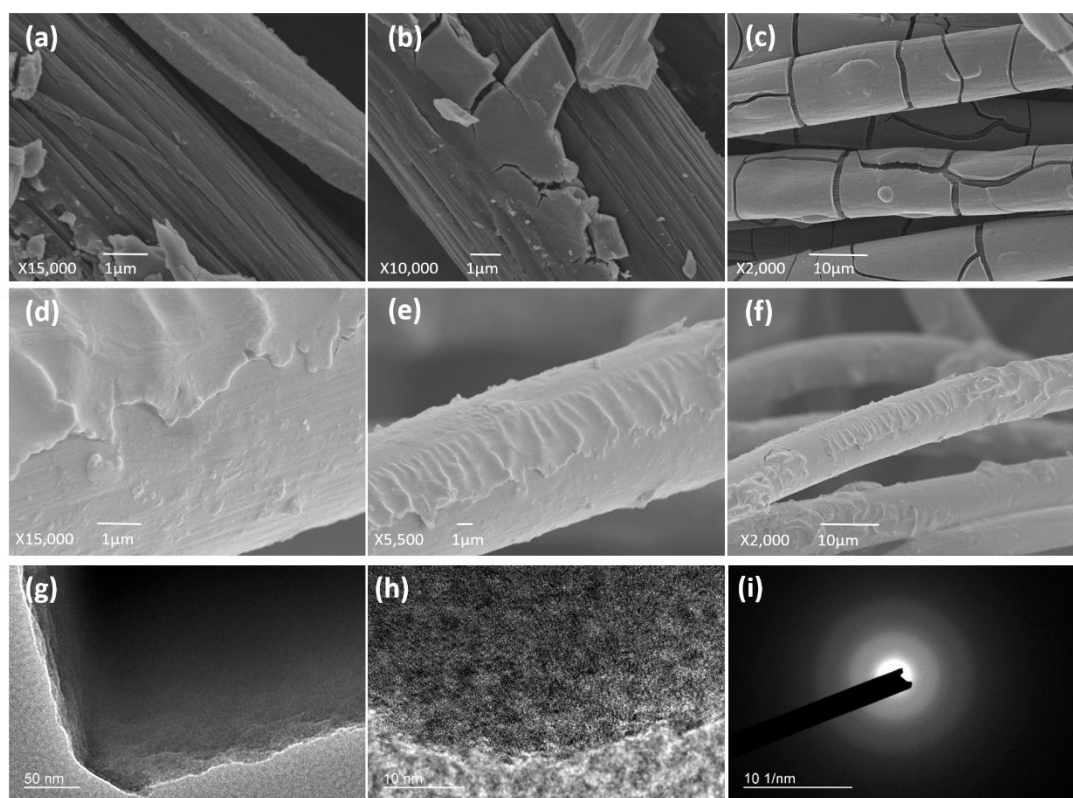


**Fig.1** (a-c) SEM images of FeWCo<sub>3</sub>O<sub>4</sub>/CFC with different magnifications. (d-f) SEM images of FeWCo<sub>3</sub>O<sub>4</sub>/PPy/CFC with different magnifications. (g-i) TEM image, HRTEM image and corresponding SAED pattern of FeWCo<sub>3</sub>O<sub>4</sub> layer stripped from FeWCo<sub>3</sub>O<sub>4</sub>/PPy/CFC.



Fig. 1 a-c displays the SEM images of  $\text{FeWCo}_3\text{O}_4$  on the CFC without PPy modification under different magnifications. It can be seen clearly that the deposited  $\text{FeWCo}_3\text{O}_4$  layer has many cracks and is easy to be peeled off, leading to poor contact between  $\text{FeWCo}_3\text{O}_4$  layer and CFC fiber and resulting in mechanical instability of the  $\text{FeWCo}_3\text{O}_4$ /CFC structure. In contrast, when the PPy modified CFC is used as substrate, the contact between  $\text{FeWCo}_3\text{O}_4$  and substrate is significantly improved (Fig. 1 d-f). No cracks can be identified at the surface of the  $\text{FeWCo}_3\text{O}_4$ /PPy/CFC structure. The strong adhesion between  $\text{FeWCo}_3\text{O}_4$  and substrate prevents the loss of effective active sites and leads to stable catalytic performance.

The lack of distinct lattice fringes in TEM images (Fig. 1 g and h) and the diffuse rings in the corresponding selected area electron diffraction (SAED) pattern (Fig. 1 i) reveal that the thin  $\text{FeWCo}_3\text{O}_4$  nanosheets are amorphous.

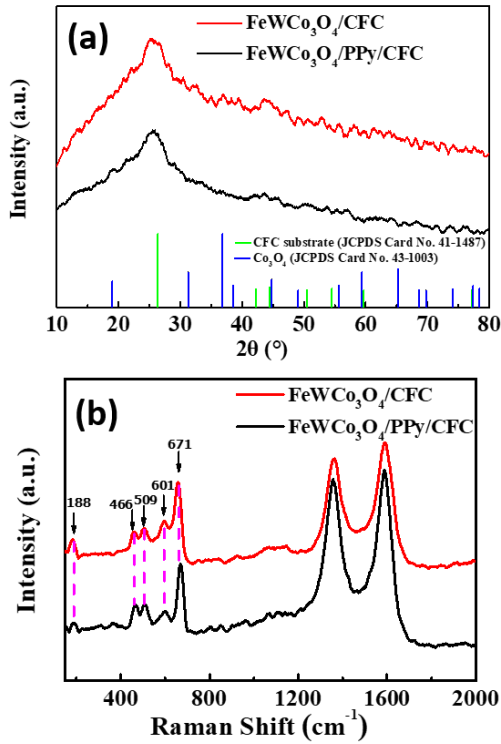


**Fig. 2** (a) XRD patterns and (b) Raman spectra of electrodeposited FeWCo<sub>3</sub>O<sub>4</sub>/PPy/CFC and FeWCo<sub>3</sub>O<sub>4</sub>/CFC.

Only diffraction peaks of the CFC substrate (JCPDS Card No. 41-1487) can be observed in the XRD pattern of the electrodeposited FeWCo<sub>3</sub>O<sub>4</sub> (Fig. 2a), which further confirms the amorphous structure of the FeWCo<sub>3</sub>O<sub>4</sub> layer. The Raman spectrum reveals the existence of Co<sub>3</sub>O<sub>4</sub> as shown in Fig. 2b. The observed 188, 466, 509, 601, and 671 cm<sup>-1</sup> peaks agree well with pure spinel structure of Co<sub>3</sub>O<sub>4</sub> [29]. The two peaks at 1360 and 1590 cm<sup>-1</sup> belong to the CFC substrate.

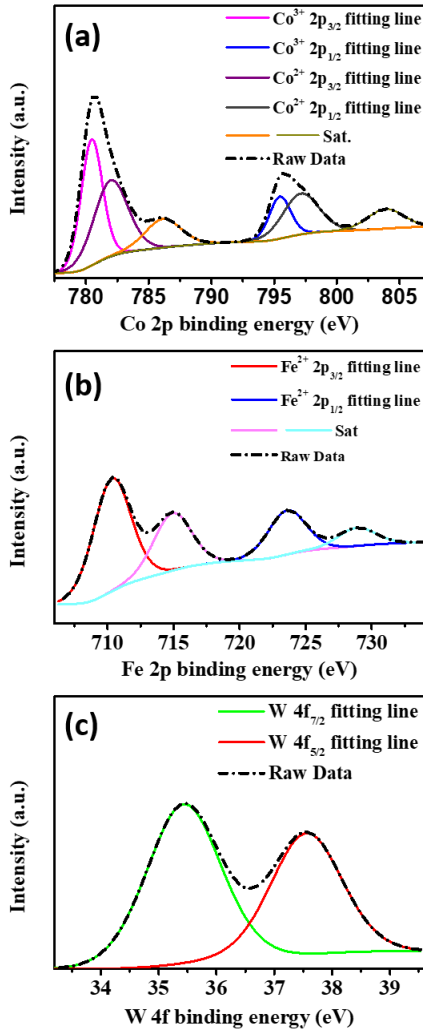


**Fig. 3** Measurements of (a) Co 2p XPS, (b) Fe 2p XPS, (c) W 4f XPS of FeWCo<sub>3</sub>O<sub>4</sub>/PPy/CFC.

XPS spectrum provides the detailed information of valence states. Co in Co<sub>3</sub>O<sub>4</sub> is actually in a mixed oxidation state of Co<sup>2+</sup> and Co<sup>3+</sup>. As shown in Fig. 3a, Co consists of +2 and +3 values which is consistent with Co<sub>3</sub>O<sub>4</sub> composition indicated by Raman spectra. The peaks at 780.48 and 782.03 eV belong to Co 2p<sub>3/2</sub> region of Co<sup>3+</sup> and Co<sup>2+</sup>, respectively. The corresponding satellite peak of Co 2p<sub>3/2</sub> is observed at 786.23 eV. Peaks of Co 2p<sub>1/2</sub> are also observed at 795.48 eV for Co<sup>3+</sup> and 797.23 eV for Co<sup>2+</sup>,

accompanied with a satellite peak (denoted as Sat.) at 803.98 eV. Fig. 3b shows the  $\text{Fe}^{2+}$   $2p_{3/2}$  peak at 710.43 eV, with a satellite peak at 715.03 eV. Peaks at 723.73 and 729.03 eV belong to  $\text{Fe}^{2+}$   $2p_{1/2}$  and the corresponding satellite peaks, respectively. The XPS results reveal that Fe exists only in the valence state of  $\text{Fe}^{2+}$ . As shown in Fig. 3c, the peaks at 35.45 and 37.58 eV belong to W  $4f_{7/2}$  and W  $4f_{5/2}$  of  $\text{W}^{6+}$ , respectively, indicating that only  $\text{W}^{6+}$  exists in the deposited  $\text{FeWCo}_3\text{O}_4$ . EDS measurement (Fig. S1, Supporting Information) shows that the sample contains the major metal element of Co, with only small amounts Fe and W.

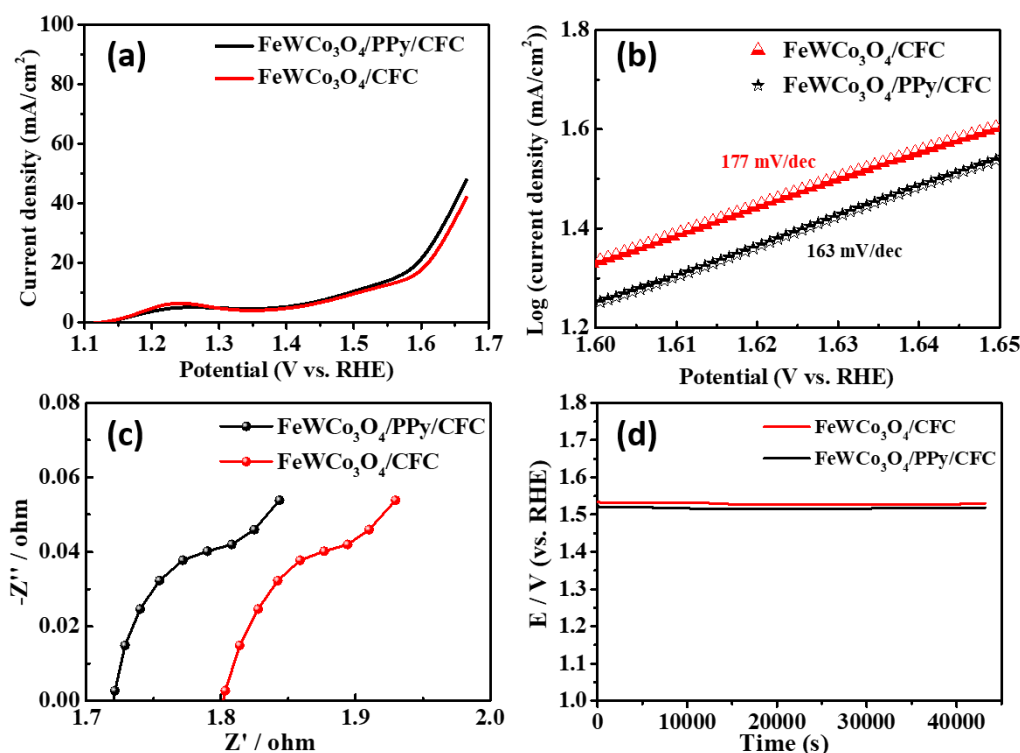


**Fig. 4** (a) Polarization curve, (b) Tafel plot, (c) EIS plot and (d) Chronopotentiometric curve of  $\text{FeWCo}_3\text{O}_4/\text{PPy}/\text{CFC}$  and  $\text{FeWCo}_3\text{O}_4/\text{CFC}$

The OER electrocatalytic property was tested in 1.0 M KOH alkaline media at a

scan rate of 2 mV s<sup>-1</sup> with SCE as reference electrode and Pt plate as counter electrode.

The potential measured with the SCE reference electrode can be converted into the potential with respect to the reversible hydrogen electrode (RHE) according to the following equation:

$$E(\text{RHE}) = E(\text{SCE}) + (0.059 \text{ pH} + 0.242) \text{ V}$$

The polarization curves of FeWCo<sub>3</sub>O<sub>4</sub>/PPy/CFC and FeWCo<sub>3</sub>O<sub>4</sub>/CFC are shown in Fig. 4a. The peaks of the polarization curves near 1.25 V (vs. RHE) may be associated with the reaction:  $\text{Co}_3\text{O}_4 + \text{H}_2\text{O} + \text{OH}^- \rightarrow 3\text{CoOOH} + e^-$ . The conductive CoOOH formed on the surface of the electrode is found to be active to the OER [30]. The current density of FeWCo<sub>3</sub>O<sub>4</sub>/PPy/CFC is higher than FeWCo<sub>3</sub>O<sub>4</sub>/CFC beyond 1.55-1.65 V (vs RHE). This can be explained by the function of PPy which can serve as a conductive binder to improve the conductivity. CV measurement indicates the existence of additional redox current from 1.25 to 1.50 V vs. RHE (Fig. S3, Fig. S4 Supporting Information). To avoid the disturbance of this redox current, the current density at an overpotential of 400 mV (1.63 V) is used to compare the electrocatalytic performance of the two samples. It can be seen that the FeWCo<sub>3</sub>O<sub>4</sub>/PPy/CFC free-standing electrode reaches a higher current density of 36.2 mA cm<sup>-2</sup> than the FeWCo<sub>3</sub>O<sub>4</sub>/CFC (30.7 mA cm<sup>-2</sup>) does at an overpotential of 400 mV. The Tafel slope of FeWCo<sub>3</sub>O<sub>4</sub>/PPy/CFC (163 mV dec<sup>-1</sup>) is slightly lower than that of FeWCo<sub>3</sub>O<sub>4</sub>/CFC (177 mV dec<sup>-1</sup>) (Fig. 4b), which can be ascribed to the enhanced electron transfer from PPy. EIS test indicates the lower resistance of FeWCo<sub>3</sub>O<sub>4</sub>/PPy/CFC than that of FeWCo<sub>3</sub>O<sub>4</sub>/CFC (Fig. 4c). The stability of FeWCo<sub>3</sub>O<sub>4</sub>/PPy/CFC and FeWCo<sub>3</sub>O<sub>4</sub>/CFC is tested by applying a

constant current density of  $10 \text{ mA cm}^{-2}$  for 12 hours (Fig. 4d). The catalytic performance is stable without obvious decay for 12 hours. Electrodeposition time is an important factor to influence the catalytic performance of  $\text{FeWCo}_3\text{O}_4/\text{PPy}/\text{CFC}$ . When the deposition time is two hours, the sample shows the best electrocatalytic performance (Fig. S2, Supporting Information). The difference in the electrocatalytic performance of samples deposited with different deposition time periods may result from two factors: the number of active sites and electron transportation. The sample with too short deposition time (one hour) may suffer from fewer active sites. However, the sample with too long deposition time (three hour) has thick layers which impedes the electron transfer.

## Conclusion

By using a simple anodic electrodeposition method, amorphous  $\text{Co}_3\text{O}_4$  co-doped with Fe, W were grown on  $\text{PPy}/\text{CFC}$  substrate. The  $\text{FeWCo}_3\text{O}_4/\text{PPy}/\text{CFC}$  electrode with additional PPy layer possesses better OER electrocatalytic activities than  $\text{FeWCo}_3\text{O}_4/\text{CFC}$ . PPy can serve as conductive binder to improve the surface contact between  $\text{FeWCo}_3\text{O}_4$  active material and the substrate. CFC is flexible and highly conductive, which is also stable at anodic condition during the deposition of  $\text{FeWCo}_3\text{O}_4$ . The synthesized  $\text{FeWCo}_3\text{O}_4/\text{PPy}/\text{CFC}$  free-standing electrode exhibits high OER catalytic performance with a current density of  $36.2 \text{ mA cm}^{-2}$  at an overpotential of 400 mV, and a Tafel slope of  $163 \text{ mV dec}^{-1}$ . This study provides new insight for design and

synthesis of highly-efficient OER catalyst.

### **Acknowledgement**

This work was supported by the Hong Kong Polytechnic University (Project No. RUKQ).

### **References**

1. Chu S, Majumdar A (2012) Opportunities and challenges for a sustainable energy future. *Nature* 488 (7411):294-303
2. Turner JA (2004) Sustainable Hydrogen Production. *Science* 305 (5686):972-974. doi:10.1126/science.1103197
3. Walter MG, Warren EL, McKone JR, Boettcher SW, Mi Q, Santori EA, Lewis NS (2010) Solar water splitting cells. *Chem Rev* 110 (11):6446-6473
4. Dresselhaus M, Thomas I (2001) Alternative energy technologies. *Nature* 414 (6861):332-337
5. Zou X, Zhang Y (2015) Noble metal-free hydrogen evolution catalysts for water splitting. *Chem Soc Rev* 44 (15):5148-5180. doi:10.1039/c4cs00448e
6. Pletcher D, Li X (2011) Prospects for alkaline zero gap water electrolyzers for hydrogen production. *Int J Hydrogen Energy* 36 (23):15089-15104
7. Reier T, Oezaslan M, Strasser P (2012) Electrocatalytic oxygen evolution reaction (OER) on Ru, Ir, and Pt catalysts: a comparative study of nanoparticles and bulk materials. *Acs Catalysis* 2 (8):1765-1772
8. Ma W, Ma R, Wang C, Liang J, Liu X, Zhou K, Sasaki T (2015) A superlattice of

alternately stacked Ni–Fe hydroxide nanosheets and graphene for efficient splitting of water. *ACS nano* 9 (2):1977-1984

9. Zhang B, Zheng X, Voznyy O, Comin R, Bajdich M, García-Melchor M, Han L, Xu J, Liu M, Zheng L, García de Arquer FP, Dinh CT, Fan F, Yuan M, Yassitepe E, Chen N, Regier T, Liu P, Li Y, De Luna P, Janmohamed A, Xin HL, Yang H, Vojvodic A, Sargent EH (2016) Homogeneously dispersed multimetal oxygen-evolving catalysts. *Science* 352 (6283):333-337. doi:10.1126/science.aaf1525

10. Lu Z, Wang H, Kong D, Yan K, Hsu PC, Zheng G, Yao H, Liang Z, Sun X, Cui Y (2014) Electrochemical tuning of layered lithium transition metal oxides for improvement of oxygen evolution reaction. *Nat Commun* 5:4345. doi:10.1038/ncomms5345

11. Maiyalagan T, Jarvis KA, Therese S, Ferreira PJ, Manthiram A (2014) Spinel-type lithium cobalt oxide as a bifunctional electrocatalyst for the oxygen evolution and oxygen reduction reactions. *Nat Commun* 5:3949. doi:10.1038/ncomms4949

12. Liu Y-C, Koza JA, Switzer JA (2014) Conversion of electrodeposited Co(OH)<sub>2</sub> to CoOOH and Co<sub>3</sub>O<sub>4</sub>, and comparison of their catalytic activity for the oxygen evolution reaction. *Electrochim Acta* 140:359-365. doi:10.1016/j.electacta.2014.04.036

13. Zhou Y, Lee CW, Kim SK, Yoon S (2012) Ordered Mesoporous Carbon/MoO<sub>2</sub> Nanocomposites as Stable Supercapacitor Electrodes. *ECS Electrochemistry Letters* 1 (1):A17-A20. doi:10.1149/2.013201eel

14. Gong M, Dai H (2014) A mini review of NiFe-based materials as highly active oxygen evolution reaction electrocatalysts. *Nano Research* 8 (1):23-39. doi:10.1007/s12274-014-0591-z

15. Seh ZW, Kibsgaard J, Dickens CF, Chorkendorff I, Norskov JK, Jaramillo TF (2017)



Combining theory and experiment in electrocatalysis: Insights into materials design. *Science* 355 (6321). doi:10.1126/science.aad4998

16. Huang J, Chen J, Yao T, He J, Jiang S, Sun Z, Liu Q, Cheng W, Hu F, Jiang Y, Pan Z, Wei S (2015) CoOOH Nanosheets with High Mass Activity for Water Oxidation. *Angew Chem Int Ed Engl* 54 (30):8722-8727. doi:10.1002/anie.201502836

17. Wang A-L, Xu H, Li G-R (2016) NiCoFe Layered Triple Hydroxides with Porous Structures as High-Performance Electrocatalysts for Overall Water Splitting. *ACS Energy Letters* 1 (2):445-453. doi:10.1021/acsenergylett.6b00219

18. Jiang N, You B, Sheng M, Sun Y (2015) Electrodeposited cobalt-phosphorous-derived films as competent bifunctional catalysts for overall water splitting. *Angew Chem Int Ed Engl* 54 (21):6251-6254. doi:10.1002/anie.201501616

19. Jiang N, You B, Sheng M, Sun Y (2016) Bifunctionality and Mechanism of Electrodeposited Nickel-Phosphorous Films for Efficient Overall Water Splitting. *ChemCatChem* 8 (1):106-112. doi:10.1002/cctc.201501150

20. Zhao S, Wang Y, Dong J, He C-T, Yin H, An P, Zhao K, Zhang X, Gao C, Zhang L, Lv J, Wang J, Zhang J, Khattak AM, Khan NA, Wei Z, Zhang J, Liu S, Zhao H, Tang Z (2016) Ultrathin metal-organic framework nanosheets for electrocatalytic oxygen evolution. *Nature Energy* 1:16184. doi:10.1038/nenergy.2016.184

21. Zhuang Z, Sheng W, Yan Y (2014) Synthesis of monodispersed Au@Co<sub>3</sub>O<sub>4</sub> core-shell nanocrystals and their enhanced catalytic activity for oxygen evolution reaction. *Adv Mater* 26 (23):3950-3955. doi:10.1002/adma.201400336

22. Zhao Y, Chen S, Sun B, Su D, Huang X, Liu H, Yan Y, Sun K, Wang G (2015) Graphene-Co<sub>3</sub>O<sub>4</sub> nanocomposite as electrocatalyst with high performance for oxygen evolution reaction. *Sci Rep* 5:7629. doi:10.1038/srep07629

23. Han X, Yu C, Zhou S, Zhao C, Huang H, Yang J, Liu Z, Zhao J, Qiu J (2017) Ultrasensitive Iron-Triggered Nanosized Fe-CoOOH Integrated with Graphene for Highly Efficient Oxygen Evolution. *Advanced Energy Materials*:1602148. doi:10.1002/aenm.201602148
  
24. Shang C, Li M, Wang Z, Wu S, Lu Z (2016) Electrospun Nitrogen-Doped Carbon Nanofibers Encapsulating Cobalt Nanoparticles as Efficient Oxygen Reduction Reaction Catalysts. *ChemElectroChem* 3 (9):1437-1445. doi:10.1002/celec.201600275
  
25. Liu Y, Liu Y, Cheng SH-S, Yu S, Nan B, Bian H, Md K, Wang M, Chung CY, Lu Z-G (2016) Conformal Coating of Heterogeneous CoO/Co Nanocomposites on Carbon Nanotubes as Efficient Bifunctional Electrocatalyst for Li-Air Batteries. *Electrochim Acta* 219:560-567. doi:10.1016/j.electacta.2016.10.064
  
26. Unni SM, Dhavale VM, Pillai VK, Kurungot S (2010) High Pt Utilization Electrodes for Polymer Electrolyte Membrane Fuel Cells by Dispersing Pt Particles Formed by a Preprecipitation Method on Carbon “Polished” with Polypyrrole. *The Journal of Physical Chemistry C* 114 (34):14654-14661. doi:10.1021/jp104664t
  
27. Bashyam R, Zelenay P (2006) A class of non-precious metal composite catalysts for fuel cells. *Nature* 443 (7107):63-66. doi:10.1038/nature05118
  
28. Olson TS, Pylypenko S, Atanassov P, Asazawa K, Yamada K, Tanaka H (2010) Anion-Exchange Membrane Fuel Cells: Dual-Site Mechanism of Oxygen Reduction Reaction in Alkaline Media on Cobalt–Polypyrrole Electrocatalysts. *The Journal of Physical Chemistry C* 114 (11):5049-5059. doi:10.1021/jp910572g
  
29. Diallo A, Beye AC, Doyle TB, Park E, Maaza M (2015) Green synthesis of Co<sub>3</sub>O<sub>4</sub> nanoparticles via *Aspalathus linearis*: Physical properties. *Green Chemistry Letters and Reviews* 8 (3-4):30-36. doi:10.1080/17518253.2015.1082646

30. Wang HY, Hung SF, Chen HY, Chan TS, Chen HM, Liu B (2016) In Operando Identification of Geometrical-Site-Dependent Water Oxidation Activity of Spinel  $\text{Co}_3\text{O}_4$ . *J Am Chem Soc* 138 (1):36-39. doi:10.1021/jacs.5b10525